Interaction of Soluble Guanylate Cyclase with YC-1: Kinetic and Resonance Raman Studies†

John W. Denninger,‡ Johannes P. M. Schelvis,§ Philip E. Brandish,|| Yunde Zhao,‡ Gerald T. Babcock,*,§ and Michael A. Marletta*,‡,||,⊥

Department of Biological Chemistry, Medical School, Howard Hughes Medical Institute and Interdepartmental Program in Medicinal Chemistry, College of Pharmacy, University of Michigan, Ann Arbor, Michigan 48109-0606, and Department of Chemistry and the LASER Laboratory, Michigan State University, East Lansing, Michigan 48824-1322

Received October 7, 1999; Revised Manuscript Received February 2, 2000

ABSTRACT: The enzyme-soluble guanylate cyclase (sGC), which converts GTP to cGMP, is a receptor for the signaling agent nitric oxide (NO). YC-1, a synthetic benzylindazole derivative, has been shown to activate sGC in an NO-independent fashion. In the presence of carbon monoxide (CO), which by itself activates sGC approximately 5-fold, YC-1 activates sGC to a level comparable to stimulation by NO alone. We have used kinetic analyses and resonance Raman spectroscopy (RR) to investigate the interaction of YC-1 and CO with guanylate cyclase. In the presence of CO and 200 μM YC-1, the $V_{max}/K_{m\ GTP}$ increases 226-fold. While YC-1 does not perturb the RR spectrum of the ferrous form of baculovirus/Sf9 cell expressed sGC, it induces a shift in the Fe−CO stretching frequency for the CO-bound form from 474 to 492 cm^{-1}. Similarly, YC-1 has no effect on the RR spectrum of ferrous $\beta1_{1-385}$, the isolated sGC heme-binding domain, but shifts the ν(Fe−CO) of CO-$\beta1_{1-385}$ from 478 to 491 cm^{-1}, indicating that YC-1 binds in heme-binding region of sGC. In addition, the CO-bound forms of sGC and $\beta1_{1-385}$ in the presence of YC-1 lie on the ν(Fe−CO) vs ν(C−O) correlation curve for proximal ligands with imidazole character, which suggests that histidine remains the heme proximal ligand in the presence of YC-1. Interestingly, YC-1 does not shift ν(Fe−CO) for the CO-bound form of H105G(Im), the imidazole-rescued heme ligand mutant of $\beta1_{1-385}$. The data are consistent with binding of CO and YC-1 to the sGC heme-binding domain leading to conformational changes that give rise to an increase in catalytic turnover and a change in the electrostatic environment of the heme pocket.

Soluble guanylate cyclase (sGC)[1] is an integral part of the nitric oxide (·NO)/cyclic guanosine monophosphate (cGMP) signaling system (for recent reviews, see *1, 2*). sGC catalyzes the conversion of guanosine triphosphate (GTP) to the second messenger, cGMP. The rate of this conversion is increased more than 400-fold in the presence of ·NO. sGC is a hemoprotein; in fact, it is the binding of ·NO to the tightly bound sGC heme that brings about enzyme activation. sGC is composed of two subunits, α and β, which, on the basis of amino acid sequence alignments, appear to be descended from a common ancestral gene. The COOH-terminal regions of the two subunits, which share sequence homology to regions in the particulate sGC and the adenylate cyclases, are thought to compose the sGC catalytic domain. The NH_2-terminal region of the β subunit has been shown to bind the heme prosthetic group (*3*−*5*), whereas the function of the NH_2-terminal region of the α subunit is unknown. Although sGC has been studied for many years, it is only now that the molecular details of its activation by ·NO are becoming clear.

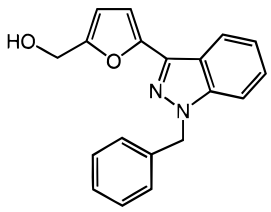

FIGURE 1: Chemical structure of YC-1. "YC-1" is the Yung Shin Pharmaceutical Industry Co. name for 3-(5′-hydroxymethyl-2′-furyl)-1-benzylindazole.

YC-1, or 3-(5′-hydroxymethyl-3′-furyl)-1-benzylindazole (Figure 1), a novel activator of sGC, was first shown to inhibit platelet aggregation, to disaggregate platelets, and to prolong bleeding times in mice (*6*). Additional findings, all consistent with known pathways involving sGC, showed that YC-1 inhibits proliferation of vascular smooth muscle cells (*7*), relaxes vascular smooth muscle (*8*−*10*), and inhibits

† This work was supported by the Howard Hughes Medical Institute, the Searle Chair Endowment Fund, and NIH Grant GM25480.

* To whom correspondence should be addressed.

‡ Department of Biological Chemistry, University of Michigan.

§ Department of Chemistry and the LASER Laboratory, Michigan State University.

|| Division of Medicinal Chemistry, University of Michigan.

⊥ Howard Hughes Medical Institute, University of Michigan.

[1] Abbreviations: $\beta1_{1-385}$, residues 1−385 of the β1 subunit of sGC; cGMP, guanosine 3′,5′-cyclic monophosphate; CO, carbon monoxide; CO-$\beta1_{1-385}$, CO-bound form of $\beta1_{1-385}$; CO-sGC, CO-bound form of sGC; CO-H105G(Im), ferrous CO-bound form of H105G(Im); DEA-NO, diethylamine NONOate; DMSO, dimethyl sulfoxide; DTT, 1,4-dithiothreitol; GTP, guanosine 5′-triphosphate; H105G, $\beta1_{1-385}$ H105G mutant; H105G(Im), H105G purified and expressed in the presence of imidazole with heme bound; Im, imidazole; ν(CO), C−O stretching frequency; ν(Fe−CO), Fe−CO stretching frequency; ν(Fe−His), Fe−His stretching frequency; ·NO, nitric oxide; ·NO-sGC, ·NO-bound form of sGC; RR, resonance Raman spectroscopy; sGC, soluble guanylate cyclase; TEA, triethanolamine; YC-1, 3-(5′-hydroxymethyl-3′-furyl)-1-benzylindazole.

10.1021/bi992332q CCC: $19.00
Published on Web 03/14/2000

platelet function (*11*−*13*). Subsequent work (*10, 14*−*16*) demonstrated that YC-1 activated sGC directly, without the intermediate production of ·NO or some other factor capable of activating sGC. Also, YC-1 alone was shown to activate sGC 6−12-fold (*10, 14, 15*). In the presence of ·NO, YC-1 caused at best a small activation (0.9−1.4-fold above ·NO alone; *10, 14, 15*); however, in the presence of CO, YC-1 caused a large activation (31−34-fold above CO alone) and raised the specific activity to the same level as the ·NO-stimulated enzyme (*14, 15*). CO and YC-1, therefore, were found to synergistically activate sGC. It is instructive to compare the isolated effect of YC-1 on activation by CO and ·NO: In the absence of YC-1, there is a 4-fold activation by CO and a 200-fold activation by ·NO over basal activity; in its presence, levels of activation by CO and ·NO over YC-1 alone are virtually identical (averaging 20-fold, depending on the protein preparation) (*14, 15*).

Interestingly, YC-1 was not found to alter the Soret maximum of sGC or CO-sGC (*15, 16*). One group has reported a shift from 424 to 421 nm in the presence of GTP (*17*); however, given the reported concentrations of YC-1 and DMSO, scattering due to precipitated YC-1 may have contributed to the shift. In any case, the lack of a significant shift indicated that the sGC heme iron underwent no changes (i.e., changes in heme coordination number, oxidation state, and spin state) in the presence of YC-1. Despite the large activation of CO-sGC by YC-1, this form of the enzyme appeared to remain 6-coordinate in the presence of YC-1. This observation suggested that YC-1 might activate CO-sGC without cleaving the Fe−His bond, which is broken by the binding of ·NO; alternatively, the Fe−His bond might break and re-form with a different histidine residue. Another possible explanation for the effect of YC-1 on CO-sGC is that YC-1 raises the affinity of the sGC heme for CO; however, in the presence of saturating concentrations of CO, YC-1 could not be acting in this way. Alternatively, the binding of CO to the sGC heme may increase the affinity of the interaction with YC-1. Whereas stopped-flow spectrophotometry experiments in our laboratory indicated no change in the on- and off-rates for CO in the presence of YC-1, and thus no change in the K_d for CO (*15*), there have been reports of decreases in the EC_{50} for both CO and ·NO caused by the addition of YC-1 (*14, 17*).

In the work reported here, kinetic analyses show that YC-1 is a mixed-type activator (changes in K_m and V_{max}) for sGC, CO-sGC, and ·NO-sGC and that YC-1 increases the "efficiency" (V_{max}/K_m) of CO-sGC over 200-fold. Resonance Raman spectroscopy of the ferrous and CO-bound forms of sGC, $\beta 1_{1-385}$ and H105G(Im), in the presence of YC-1 reveals that YC-1 (1) induces no RR visible changes in the heme environment of the ferrous forms, (2) shifts the Fe−CO stretching frequency of CO-sGC and CO-$\beta 1_{1-385}$, but not that of CO-H105G(Im), (3) likely leaves the proximal histidine ligand intact, and (4) induces conformational changes in the catalytic domain that lead to an increase in catalytic activity and in the heme domain that result in changes in the electrostatic environment of the heme pocket.

MATERIALS AND METHODS

Materials. Unless otherwise indicated, all reagents were purchased from Sigma Chemical Co. Diethylamine NONOate (DEA-NO) was purchased from Cayman Chemical Co. YC-1, synthesized as described (*18*), was a generous gift from Dr. Che-Ming Teng (National Taiwan University). Heterodimeric sGC (rat $\alpha 1\beta 1$) was expressed using the baculovirus/Sf9 expression system and purified using revised methods based on those described previously (*19*). The heme domain of sGC ($\beta 1_{1-385}$) and the heme ligand mutant (H105G) were expressed in *E. coli* and purified as described previously (*4, 5*).

Activity Assays. End-point assays were performed as described (*20*); standard components included 50 mM TEA, pH 7.4, 5 mM DTT, 5 mM $MgCl_2$, and 1.5 mM GTP. Assays were quenched by the precipitation of substrate with 400 μL of 125 mM $Zn(CH_3COO)_2$ and 500 μL of 125 mM Na_2CO_3. Quench mixtures were cleared of precipitate by centrifugation prior to product detection. Product was detected using a cGMP enzyme immunoassay kit (BioMol), following the manufacturer's instructions. For the purpose of activity assays, sGC was stored in 40% (v/v) glycerol in sealed vials under nitrogen at −80 °C. DEA-NO was added as a 10 mM stock in 10 mM NaOH, to give a final concentration of 1 mM in the assay. The assay pH was not altered by addition of the DEA-NO solution. Activation with 1 mM DEA-NO was compared to activation with 1% ·NO gas, purified by bubbling through concentrated KOH, and found to be identical; in contrast, 100 μM sodium nitroprusside produced activation approximately 60% of that produced by ·NO gas. CO was added to assays before the preincubation with a gastight syringe by bubbling approximately 75 μL of CO gas through the assay solution and forming an approximately 25 μL bubble of CO gas underneath the assay solution (in the vertex of each eppendorf tube). This method of CO addition was compared to assaying the enzyme under a 100% CO atmosphere in gastight vials and found to give identical levels of activation.

K_m and V_{max} determinations were performed for each form of the enzyme at 200, 100, 50, 25, and 0 μM YC-1. For sGC, GTP concentrations ranged from 9.4 to 1200 μM; for CO-sGC and ·NO-sGC, GTP concentration ranged from 6.3 to 800 μM. For each experiment, the sGC sample was thawed, diluted to an appropriate concentration in 150 mM TEA, pH 7.4, and used to initiate the reaction. To ensure that activity remained linear during the 2 min reactions over the entire range of GTP concentrations, separate assays were performed in which aliquots were withdrawn and quenched at 30 s intervals for the highest and lowest GTP concentrations. To control for the effect of DMSO addition, serial dilutions of YC-1 were prepared in DMSO, and a constant volume (and thus a constant v/v percentage) of DMSO or DMSO/YC-1 was added to each assay within an experimental series. Because of the low aqueous solubility of YC-1, concentrations of DMSO up to 4% v/v were required to maintain YC-1 in solution.

Resonance Raman Spectroscopy. Resonance Raman spectra were recorded using samples of 110−150 μL in a quartz spinning cell sealed with a rubber septum that was cooled to approximately 10 °C with a stream of cooled N_2. Ferrous samples were placed under an argon atmosphere, and ferrous-CO samples were placed under a CO atmosphere. The ferrous-CO complex of H105G-Im, which is isolated in its ferric form, was prepared by reducing the sample with dithionite under a CO atmosphere. For all samples, formation

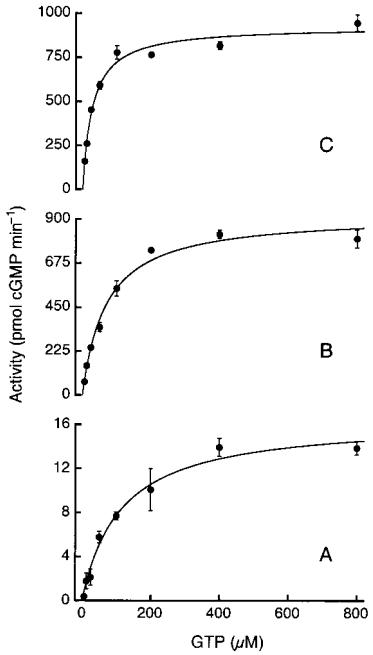

FIGURE 2: Effect of increasing YC-1 concentration on the V_{max} and $K_{m\ GTP}$ of CO-sGC. CO-sGC activity vs GTP concentration in the presence of (A) 0 μM, (B) 25 μM, and (C) 100 μM YC-1. Because it is identical for the three panels, the *x*-axis is shown only in panel A. Assays were performed as described under Materials and Methods. Each point represents the mean ± range/2 for duplicate 2 min assays; cGMP concentrations for each individual assay were also determined in duplicate. Fitting the data for each YC-1 concentration to activity = V_{max}[GTP]/($K_{m\ GTP}$ + [GTP]) yields the solid curves shown in each panel.

of the desired complex was monitored by electronic absorption spectroscopy both before and after acquisition of resonance Raman spectra. No sample degradation was observed after the Raman experiments. The resonance Raman spectra of ferrous sGC in the presence and absence of YC-1 were obtained with 431 nm excitation using a dye laser (Coherent 599) with stilbene 420 as the dye, pumped with the UV output of an Ar^+ laser (Coherent Innova 200). All other spectra were recorded with an excitation wavelength of 413.1 nm, using a Kr^+ laser (Coherent K-90). Resonance Raman scattering was detected with a Spex 1877 Triplemate spectrometer in combination with a liquid nitrogen cooled CCD detector (EG&G OMA 4, model 1530-CUV-1024S). Laser power was less than 1 mW for CO experiments to avoid accumulation of the CO photolysis product and approximately 10 mW for experiments with the ligand-free species. Accumulation times were typically between 0.5 and 1.5 h.

RESULTS

Kinetic Analysis. To determine the changes in both K_m and V_{max} induced by increasing concentrations of YC-1 on sGC, CO-sGC, and ·NO-sGC, K_m and V_{max} determinations were performed for each form of the enzyme. In preliminary experiments, DMSO (≤4% v/v) was shown to induce a small activation of sGC (<1.5-fold); to control for this effect, all of the assays within an experimental series were done with a constant DMSO percentage. In addition, assays were found to be linear over the 2 min assay period for both the highest and lowest concentrations of GTP (data not shown). As shown in Figure 2, increasing concentrations of YC-1 both increase the V_{max} and lower $K_{m\ GTP}$ for sGC, CO-sGC, and ·NO-sGC. Table 1 shows $K_{m\ GTP}$ in the presence and absence of YC-1 and the fold-increase induced by YC-1 for both V_{max} and $V_{max}/K_{m\ GTP}$.

Table 1: YC-1-Induced Changes in Kinetic Parameters of sGC[a]

	$K_{m\ GTP}$ (μM)		fold-increase (+YC-1/−YC-1)[b]	
	−YC-1	+YC-1	V_{max}	$V_{max}/K_{m\ GTP}$
sGC	130 ± 20	32 ± 4	4	16
CO-sGC	113 ± 19	28 ± 4	56	226
·NO-sGC	44 ± 2	14 ± 1	1.2	4

[a] For values determined in the presence of YC-1, the YC-1 concentration was 100 μM. [b] To allow comparison of V_{max} and $V_{max}/K_{m\ GTP}$ values across experiments conducted with different batches of sGC, values are given as unitless ratios of the values in the presence of YC-1 divided by values in the absence of YC-1, namely, $(V_{max})_{+YC-1}/(V_{max})_{-YC-1}$ and $(V_{max}/K_{m\ GTP})_{+YC-1}/(V_{max}/K_{m\ GTP})_{-YC-1}$.

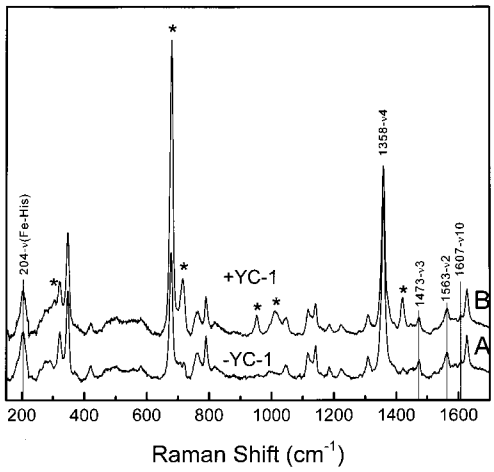

FIGURE 3: Resonance Raman spectrum of 5 μM native sGC overexpressed using the baculovirus/Sf9 expression system in the absence (A) and presence (B) of 200 μM YC-1 and 2.5% DMSO (v/v). The excitation wavelength was 431 nm, and the laser power incident on the sample was approximately 10 mW. Contributions of DMSO are indicated with an asterisk, and the broad band around 1650 cm^{-1} arises from water.

Ferrous sGC. The resonance Raman spectrum of native sGC expressed using the baculovirus/Sf9 expression system is shown in Figure 3A. We used 431 and 413.1 nm (data not shown) excitation to collect the spectrum. Both excitation wavelengths gave the same result except for differences in Raman intensities due to the resonance Raman effect. Soret excitation enhances vibrations that give insight into heme structure (*21*−*23*). The oxidation and coordination state of the heme can be determined from the π-electron density marker, ν_4, which reflects the oxidation state of the heme iron, and the spin and coordination state markers, ν_3, ν_2, ν_{10}, which are sensitive to the core size of the heme macrocycle (*23*). The spectrum of native sGC is very similar to that of native sGC isolated from bovine lung tissue (*24, 25*). The heme skeletal vibrations ν_2, ν_3, ν_4, and ν_{10} are observed at 1563, 1473, 1358, and 1607 cm^{-1}, respectively. The frequencies of these vibrations indicate that native sGC contains a 5-coordinate, high-spin ferrous heme (*22*). Furthermore, the Fe−His stretching vibration [ν(Fe−His)] is observed at 204 cm^{-1}, which is also at the same frequency as observed in native sGC from bovine lung tissue. Neither 431 nm nor 413.1 nm excitation showed evidence of the presence of a 6-coordinate, low-spin ferrous heme in native sGC, which

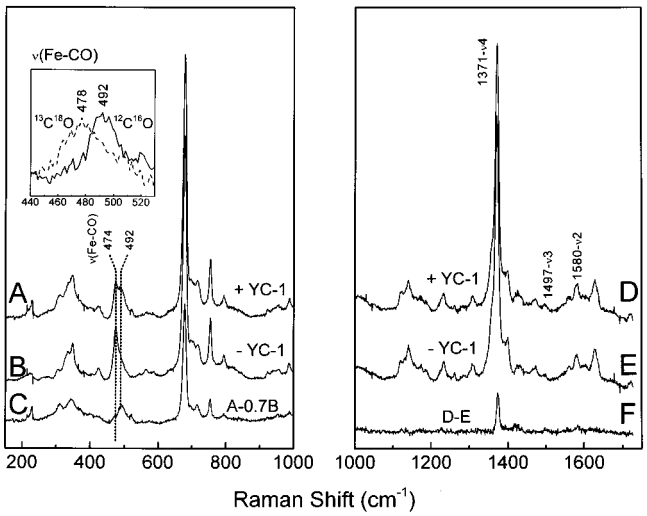

FIGURE 4: Low- and high-frequency resonance Raman spectra of CO-sGC in the presence (A and D) and absence (B and E) of 200 μM YC-1 and 2% (v/v) DMSO. (C) is the scaled low-frequency difference spectrum (A − 0.7 × B) that is the pure CO-sGC/YC-1 spectrum without contributions from CO-sGC. (F) is the normalized high-frequency difference spectrum, D − E. In this case, a scaled subtraction was not possible, because no YC-1-sensitive vibration is present in the high-frequency spectrum. Inset: The ν(Fe−CO) region of CO-sGC: $^{12}C^{16}O$ with 200 μM YC-1 (solid line), $^{13}C^{18}O$ with 200 μM YC-1 (dashed line).

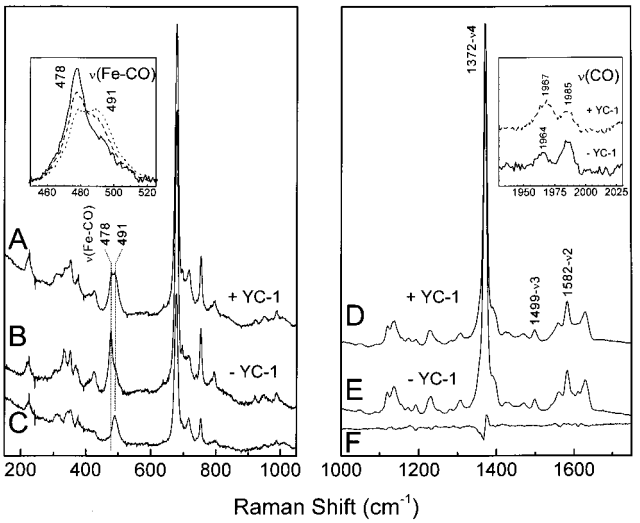

FIGURE 5: Low- and high-frequency resonance Raman spectra of CO-$\beta 1_{1-385}$ in the presence (A and D) and absence (B and E) of 200 μM YC-1 and 5% (v/v) DMSO (A) or 2.5% DMSO (D). (C) is the scaled low-frequency difference spectrum (A − 0.5 × B) that is the pure CO-$\beta 1_{1-385}$/YC-1 spectrum without contributions from CO-$\beta 1_{1-385}$. (F) is the normalized high-frequency difference spectrum, D − E. In this case, a scaled subtraction was not possible, because no YC-1-sensitive vibration is present in the high-frequency spectrum. Inset (left panel), the ν(Fe−CO) region: CO-$\beta 1_{1-385}$ in the presence of 0 μM (solid line), 100 μM (dotted line), and 200 μM (dashed line) YC-1, with 0%, 4%, and 5% DMSO, respectively. Inset (right panel), the ν(CO) region: CO-$\beta 1_{1-385}$ in the absence (solid line) and presence (dashed line) of 200 μM YC-1 and 2.5% DMSO.

has been reported by two different groups (*26*, *27*). The resonance Raman spectrum of sGC in the presence of 200 μM YC-1 and 2.5% DMSO (v/v) is shown in Figure 3B and is very similar to the spectrum of native sGC without YC-1 present. The only clear differences that are observed can be assigned to the vibrations of DMSO, which is necessary to dissolve YC-1 in aqueous solution. Neither the heme macrocycle vibrations nor ν(Fe−His) are affected by the presence of YC-1.

CO-sGC. The resonance Raman spectra of CO-sGC in the presence and absence of YC-1 are shown in Figure 4. In the absence of YC-1, the resonance Raman CO-sGC spectrum for the baculovirus/Sf9-expressed sGC (Figure 4, B and E) is almost identical to the spectrum for the bovine lung enzyme (*25*). The heme skeletal vibrations, ν_2, ν_3, and ν_4, are observed at 1580, 1497, and 1371 cm^{-1}, respectively, indicating that the heme iron is ferrous, 6-coordinate, and low spin. The Fe−CO stretching vibration [ν(Fe−CO)] is observed at 474 cm^{-1}. The 2 cm^{-1} increase in ν(Fe−CO) in the baculovirus/Sf9-expressed sGC may be due to small differences between rat and bovine lung sGC. As shown in Figure 4, YC-1 does change the resonance Raman spectrum of CO-sGC. Although no changes were detected in the high-frequency region, in the low-frequency region, ν(Fe−CO) clearly shifts from 474 to 492 cm^{-1} in a significant fraction of CO-sGC in the presence of 200 μM YC-1 and 2% DMSO. Control experiments indicate that DMSO alone does not induce this shift (data not shown). Both the existing band at 474 cm^{-1} and the new one at 492 cm^{-1} were isotope-sensitive and shifted to 464 and 478 cm^{-1}, respectively, in the presence of $^{13}C^{18}O$ (Figure 4 inset). This suggests that the heme environment is perturbed in the presence of YC-1 and that the perturbation affects the Fe−CO unit, changing ν(Fe−CO) to 492 cm^{-1}. It is important to note that maximum synergistic activation of CO-sGC is observed at a YC-1 concentration of 200 μM, while our data show that at such a concentration less than 50% of CO-sGC has changed its conformation. The small changes in the 300−400 cm^{-1} region are convoluted with contributions from DMSO. Since we do not observe any changes in the high-frequency modes of CO-sGC in the presence of YC-1, we conclude that the heme iron is still ferrous, 6-coordinate, and low spin.

$\beta 1_{1-385}$. To determine whether YC-1 interacts with the sGC heme-binding domain, the resonance Raman spectrum of $\beta 1_{1-385}$ was determined in the presence and absence of YC-1 (data not shown). As in the case of heterodimeric sGC, we did not observe any changes in either the heme macrocycle vibrations or ν(Fe−His) in the resonance Raman spectrum of ferrous $\beta 1_{1-385}$ in the presence of YC-1. In Figure 5, we show that the resonance Raman spectrum of CO-$\beta 1_{1-385}$ does, in fact, change in the presence of YC-1. As with CO-sGC, the high frequency was not affected, and the heme iron was 6-coordinate, low spin, and ferrous, which was indicated by the frequencies of ν_2, ν_3, and ν_4 at 1582, 1499, and 1372 cm^{-1}, respectively. The small difference signal near 1365 cm^{-1} may be induced by a small amount of CO photolysis product in the spectrum taken in the absence of YC-1. In the low-frequency region, ν(Fe−CO) shifted from 478 to 491 cm^{-1} in the presence of 100 μM YC-1 and 4% DMSO. Control experiments showed that DMSO alone did not induce the shift in ν(Fe−CO) (data not shown). Both the peak at 478 cm^{-1} and the shoulder at 491 cm^{-1} were isotope-sensitive, indicating that YC-1 induces a new heme pocket conformation that affects ν(Fe−CO) in $\beta 1_{1-385}$. We were also able to demonstrate that increasing the YC-1 concentration from 100 to 200 μM resulted in a decrease in the proportion of conformations with ν(Fe−CO) at 478 cm^{-1} and an increase in the proportion of conformations with

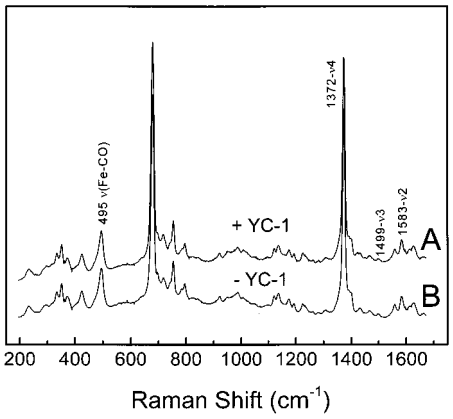

FIGURE 6: Resonance Raman spectra of H105G(Im)-CO in the absence (B) and presence (A) of 200 μM YC-1 and 5% (v/v) DMSO.

ν(Fe−CO) at 491 cm^{-1} (low-frequency inset of Figure 5). This observation supports the existence of a direct correlation between the presence of YC-1 and the appearance of a conformation of CO-sGC with ν(Fe−CO) at 491 cm^{-1}. Furthermore, both conformations of the Fe−CO unit are observed in equal amounts at 200 μM YC-1, at which concentration the synergistic activation of CO-sGC is nearly maximized. Again, we observe small differences in the 300−400 cm^{-1} region, which are convoluted with the DMSO contributions (see above). Finally, as shown in the high-frequency inset of Figure 5, the C−O stretching frequency [ν(CO)] shifts from 1985 to 1967 cm^{-1} in the presence of 200 μM YC-1.

$\beta 1_{1-385}$ H105G(Im). In Figure 6, the resonance Raman spectrum of the ferrous-CO complex of H105G(Im) is shown. It has previously been shown that in this mutant of the $\beta 1_{1-385}$ heme domain ν(Fe−CO) is shifted from that of CO-$\beta 1_{1-385}$ (*28*). The resonance Raman spectra of the ferrous-CO complex of H105G(Im) in the presence and absence of 200 μM YC-1 reveal that, in contrast to the wild-type $\beta 1_{1-385}$, YC-1 does not shift any vibrational mode including ν(Fe−CO). This indicates that CO-H105G(Im) also maintains a 6-coordinate, low-spin, ferrous heme iron in the presence of YC-1. Interestingly, in the presence of YC-1, ν(Fe−CO) shifts to 492 cm^{-1} in both CO-sGC and CO-$\beta 1_{1-385}$, while ν(Fe−CO) remains unchanged at 495 cm^{-1} in CO-H105G-(Im).

DISCUSSION

Activation. As the kinetic analysis in this work has shown, YC-1 and CO together influence the $K_{m\ GTP}$ and V_{max} of sGC in a manner strikingly analogous to ·NO, namely, by decreasing the $K_{m\ GTP}$ and increasing the V_{max} (in other words, by acting as a mixed-type activator). This result suggests that the conformational change brought about by YC-1 in the sGC heme-binding domain may well be identical to the conformational change brought about by ·NO.

Ferrous sGC and $\beta 1_{1-385}$. The resonance Raman spectrum in Figure 3A shows that rat lung sGC overexpressed using the baculovirus/Sf9 system is almost identical to that of sGC isolated from bovine lung. In both cases, the protein contains a 5-coordinate, high-spin, ferrous heme, and ν(Fe−His) occurs at the same, low frequency (*24, 25*). Other non-Raman studies have also indicated that the sGC has a 5-coordinate, high-spin ferrous heme (*20, 29*−*31*). However, in another Raman study on rat lung sGC overexpressed using baculovirus Sf9 cells, it was shown that the heme cofactor in sGC was a mixture of 5-coordinate, high-spin and 6-coordinate, low-spin (*26*). In this case, the heme was not retained during the isolation and purification steps and was reconstituted after isolation. It had been argued that the differences in heme coordination were caused by differences in isolation and purification procedures, and by protein composition. The sGC used in our present study was overexpressed using the same cDNA; except for small differences in isolation and purification procedures, the only real difference is the heme reconstitution. We have now investigated bovine lung sGC, the heme domain of rat lung sGC overexpressed in *E. coli*, and rat lung sGC overexpressed using the baculovirus/Sf9 system. In all cases, the heme was retained during isolation and purification procedures, and sGC was found to have a 5-coordinated, high-spin ferrous heme. Therefore, we conclude that the differences in the state of the heme cofactor between the two preparations of sGC overexpressed using baculovirus are most likely caused by heme reconstitution.

Our results show that there are no clear differences between the Raman spectra of sGC in the absence and presence of YC-1, even at a concentration of 200 μM at which maximum sGC activation (6-fold) has been observed. The same is observed for the $\beta 1_{1-385}$ heme domain. Since YC-1 does activate sGC 6-fold over basal activity, it must be interacting with sGC. This indicates either that YC-1 does not induce any conformational change in the sGC heme pocket that could be observed by resonance Raman spectroscopy or that the affinity of sGC for YC-1 is very low. In the latter case, the limited solubility of YC-1 in aqueous solution may reduce the magnitude of the change to below the detection limit of our Raman instrument.

YC-1 Perturbs the Heme Environment of CO-sGC. The resonance Raman spectrum of CO-sGC in the presence and absence of YC-1 revealed that YC-1 shifted the Fe−CO stretching frequency by 18 cm^{-1}, from 474 to 492 cm^{-1} (Figure 4). Although the limited solubility of YC-1 may have prevented the demonstration of a complete shift, the fact that both the peak at 474 cm^{-1} and the shoulder at 492 cm^{-1} shifted to lower frequency when $^{12}C^{16}O$ was replaced by $^{13}C^{18}O$ confirmed that YC-1's effect was on the Fe−CO stretch itself. Despite this effect on the heme environment of sGC, however, the possibility remained that YC-1 might bind to the catalytic domain (by analogy to forskolin activation of adenylate cyclase; see *15*) and influence the heme environment by a global conformational change. In other words, just as an ·NO-induced conformational change in the sGC heme-binding domain is presumed to cause an activity-raising conformational change in the sGC catalytic domain, so (in the reverse direction) might a YC-1-induced conformational change in the catalytic domain cause a heme-environment-perturbing conformational change in the heme-binding domain.

YC-1 Binds to the Heme Domain. The sGC heme domain construct, $\beta 1_{1-385}$, enabled the determination of whether YC-1 was capable of inducing the same change in the heme environment of the isolated heme-binding domain. As shown in Figure 5, YC-1 induced the same shift in Fe−CO stretch in $\beta 1_{1-385}$ as it did in heterodimeric sGC; as with the heterodimer, both peak and shoulder were isotope sensitive. Given that YC-1 induces the same heme environment

perturbation in heterodimeric sGC and in $\beta1_{1-385}$—which has no catalytic domain—we conclude that YC-1 binds to the heme-binding domain of sGC.

YC-1 Induces a Conformational Change in the Heme Pocket. The interaction between YC-1 and the sGC and $\beta1_{1-385}$ CO complexes is observed by a shift in ν(Fe−CO) from 474 and 478 cm^{-1}, respectively, to approximately 492 cm^{-1}. This shift in ν(Fe−CO) is very similar to the one previously observed in constructs of the sGC heme domain, such as H105G(Im), relative to the wild-type $\beta1_{1-385}$ (*28*). In that context, we attributed the shift to an increase in flexibility at the proximal side of the heme pocket which, in turn, allowed the formation of a hydrogen bond between CO and a distal residue in CO-H105G(Im) (*28*). Because YC-1 induces a shift of ν(Fe−CO) in CO-sGC and CO-$\beta1_{1-385}$ similar to the one we have observed previously in CO-H105G(Im) (relative to CO-$\beta1_{1-385}$), it is tempting to postulate that YC-1 acts in a similar way, namely, by allowing the formation of a hydrogen bond between CO and a distal residue. However, there are some striking differences between the two circumstances which argue against hydrogen bond formation in the presence of YC-1: (1) Our previous work has shown that the widths of ν(Fe−CO) in CO-$\beta1_{1-385}$ and CO-H105G(Im) are very similar; in other words, hydrogen bond formation does not seem to affect the width of ν(Fe−CO). In the presence of YC-1, however, the width of ν(Fe−CO) in CO-sGC and CO-$\beta1_{1-385}$ increases from about 15 cm^{-1} to about 21 cm^{-1}. This finding does not support the formation of a hydrogen bond in the presence of YC-1. (2) In CO-H105G(Im), hydrogen bond formation to CO and other small exogenous ligands, like O_2, appears to stabilize these complexes. We have proposed that stabilization of O_2 binding to the heme by hydrogen bond formation in H105G(Im) is the explanation for our finding that this form of $\beta1_{1-385}$ is sensitive to O_2 (*28*). The fact that sGC and $\beta1_{1-385}$ are both stable under aerobic conditions in the presence of YC-1 argues against YC-1 inducing hydrogen bond formation to small exogenous ligands such as CO. (3) Experiments on Mb-CO and Mb-O_2 have shown that rebinding of CO and O_2 in the 'open' form of myoglobin is faster than in its 'closed', hydrogen-bonded form (*32*). Interestingly, in CO-sGC the rebinding of CO to sGC is 3 orders of magnitude faster in the presence of YC-1 (*17*). Moreover, the fraction of the fast phase seen in these CO rebinding experiments is similar to the fraction of sGC (and $\beta1_{1-385}$) in our work that has a shifted ν(Fe−CO) in the presence of YC-1. By analogy with the closed form of myoglobin, if YC-1 induced hydrogen bond formation to CO, we would expect CO rebinding to be slower, not faster. This piece of evidence, then, also argues against the formation of a hydrogen bond to CO in the presence of YC-1.

From this analysis, therefore, we conclude that the observed shift of ν(Fe−CO) in CO-sGC and CO-$\beta1_{1-385}$ induced by YC-1 cannot be explained by the formation of a hydrogen bond between CO and a distal residue. From our results and those of others, however, we know that in the presence of YC-1: (1) ν(Fe−CO) shifts and significantly broadens, (2) sGC and $\beta1_{1-385}$ are stable under aerobic conditions, and (3) the CO recombination rate increases 1000-fold (*17*). Similar changes occur in myoglobin when its heme pocket converts from the 'closed' to the 'open' conformation, which involves displacement of the distal histidine (*32*, *33*). By analogy with myoglobin, we propose that YC-1 induces a significant conformational change in the heme pocket of CO-sGC. The structural details of this change are unknown at this point.

The changes that are observed for ν(Fe−CO) (Figures 4 and 5) and ν(C−O) (Figure 5, high-frequency inset) indicate a change in electrostatics in the distal heme pocket. The distal heme pocket in sGC has an unusual, relatively negative polarity (*25*, *34*). The changes in the CO vibrations indicate that the distal heme pocket becomes less negative. This may result from displacement of a charged distal residue or from an increase in the distance between CO and charged residues in the distal heme pocket, which would result in a change of the electrostatic field around the bound CO (*35*). The change in the electrostatics in the heme pocket of CO-sGC is opposite from that in myoglobin, in which ν(Fe−CO) shifts to a lower frequency from 508 cm^{-1} in the 'closed' conformation to 491 cm^{-1} in the 'open' conformation (*33*). Additional analysis, however, indicates that YC-1 may affect not only the distal pocket, but the proximal pocket as well. The fact that YC-1 does not have an effect on CO-H105G(Im) (see Figure 6) suggests that YC-1 interacts near the proximal side of the heme pocket: H105G(Im) does not have a covalent link with the proximal side of the heme pocket and is expected to be insensitive to changes at the proximal side. Furthermore, the proximal side of the H105G(Im) heme pocket is thought to be much less strained (*28*). Given that YC-1 has no effect on the RR spectrum of CO-H105G(Im) but does affect the spectrum of CO-sGC, it is possible that YC-1 reduces strain near the proximal heme pocket of CO-sGC. This conformational change could affect both enzyme activity and the heme pocket structure in a way similar to •NO (*36*).

The Proximal Heme Ligand in the CO Complex in the Presence of YC-1. It has been well established that both the proximal ligand and the distal heme pocket environment influence the extent of the Fe $d_\pi \rightarrow$ ligand π^* back-donation, by which ν(Fe−CO) and ν(C−O) are inversely correlated (*37*−*39*). It is known, furthermore, that the proximal ligand can compete with distal ligands for the Fe d_{z^2} orbital, and thus different correlation curves exist for proximal ligands with different basicities. As a result, correlation curves constructed from data on CO vibrations are useful in determining the basicity of a proximal ligand. CO-$\beta1_{1-385}$, in the absence and presence of YC-1, and CO-sGC, in its absence, lie on the correlation curve that corresponds to proximal histidine ligation (see Figure 7). Therefore, it is unlikely that YC-1 induces loss or displacement of the proximal ligand with a protein-derived residue other than histidine. It is also unlikely, in our view, that YC-1 itself displaces the proximal histidine and coordinates to the heme iron, as has recently been proposed (*17*): From its structure (Figure 1), it is clear that YC-1 could coordinate to the heme either through the hydroxymethyl or the furyl oxygens or through the 2-nitrogen of the indazole ring. The hydroxymethyl group has a $pK_a > 10$; therefore, this moiety will not be ionized at the pH of our samples (pH 7.4). Neutral oxygens are weak ligands that dissociate upon CO coordination, resulting in 5-coordinated CO complexes (*40*, *41*), which would contradict our results. Coordination of YC-1 to the heme with the indazole nitrogen is possible but seems unlikely given the bulky structure of YC-1. A very large

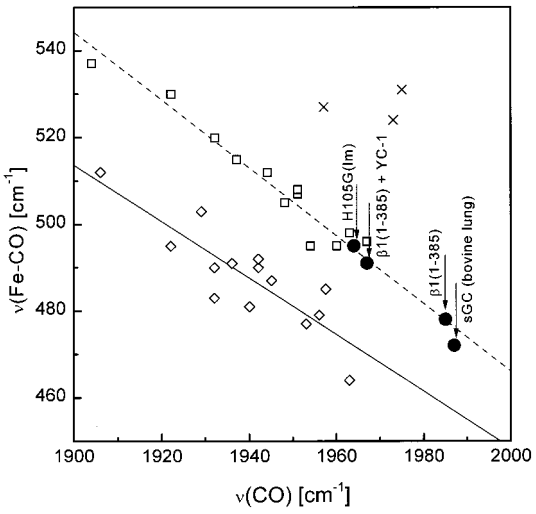

FIGURE 7: Plot of ν(Fe−CO) versus ν(CO). The dashed line is the correlation curve for proximal ligands with imidazole character. The solid line is the correlation curve for proximal ligands with thiolate and imidazolate character. Data points taken from (*25, 28, 34, 40*−*43*): square (□) = imidazole/histidine, diamond (◇) = thiolate/imidazolate, cross (×) = 5-coordinated CO complex, circle (●) = sGC (*25, 34*), $\beta1_{1-385}$ (*28*, this work), H105G(Im) (*28*, this work), and $\beta1_{1-385}$ + 200 μM YC-1 (this work).

conformational change would have to occur to accommodate YC-1 as the proximal heme ligand. The possibility remains that YC-1 leads to the substitution of a different sGC histidine residue as the proximal heme ligand in place of His105; however, two histidine mutants of $\beta1_{1-385}$, H107A and H346A, still show the YC-1-induced shift of the CO vibrations (Y. Zhao, J. Schelvis, G. Babcock, and M. Marletta, unpublished results). It is, therefore, likely that the proximal histidine, His105, remains coordinated to the sGC heme in the presence of YC-1.

Conclusion. In conclusion, then, we have made the following observations: The baculovirus/Sf9 cell expressed sGC is virtually identical by RR to the bovine lung sGC and $\beta1_{1-385}$ produced in our laboratory, and, moreover, it is five-coordinate ferrous in its as-isolated state. YC-1 induces no RR−visible changes in the ferrous forms of either sGC or $\beta1_{1-385}$; however, YC-1 does induce a shift in the ν(Fe−CO) for CO-sGC and CO-$\beta1_{1-385}$. The fact that YC-1 induces the same shift for both sGC and $\beta1_{1-385}$ strongly suggests that YC-1 binds in the sGC heme-binding region. In addition, the observation that CO-sGC and CO-$\beta1_{1-385}$ remain on the correlation curve for proximal ligands with imidazole character in the presence of YC-1 suggests that YC-1 binding does not alter the heme proximal ligand in these species. Finally, we propose that binding of YC-1 to the CO-sGC heme-binding domain leads to conformational changes that give rise to an increase in catalytic turnover and affect the electrostatic environment in the heme pocket. Given the similar effects of ·NO and CO/YC-1 on the K_m and V_{max} of sGC, it is possible that there are similarities between the structural changes elucidated herein and the structural changes brought about during activation with ·NO. Further studies are in progress in our laboratory to explore this possibility.

ACKNOWLEDGMENT

We thank the members of the Marletta laboratory for their comments on the manuscript.

REFERENCES

1. Hobbs, A. J. (1997) *Trends Pharmacol. Sci. 18*, 484−491.
2. Denninger, J. W., and Marletta, M. A. (1999) *Biochim. Biophys. Acta 1411*, 334−350.
3. Wedel, B., Humbert, P., Harteneck, C., Foerster, J., Malkewitz, J., Böhme, E., Schultz, G., and Koesling, D. (1994) *Proc. Natl. Acad. Sci. U.S.A. 91*, 2592−2596.
4. Zhao, Y., Schelvis, J. P., Babcock, G. T., and Marletta, M. A. (1998) *Biochemistry 37*, 4502−4509.
5. Zhao, Y., and Marletta, M. A. (1997) *Biochemistry 36*, 15959−15964.
6. Ko, F. N., Wu, C. C., Kuo, S. C., Lee, F. Y., and Teng, C. M. (1994) *Blood 84*, 4226−4233.
7. Yu, S. M., Cheng, Z. J., Guh, J. H., Lee, F. Y., and Kuo, S. C. (1995) *Biochem. J. 306*, 787−792.
8. Wegener, J. W., Gath, I., Forstermann, U., and Nawrath, H. (1997) *Br. J. Pharmacol. 122*, 1523−1529.
9. Wegener, J. W., and Nawrath, H. (1997) *Eur. J. Pharmacol. 323*, 89−91.
10. Mülsch, A., Bauersachs, J., Schafer, A., Stasch, J. P., Kast, R., and Busse, R. (1997) *Br. J. Pharmacol. 120*, 681−689.
11. Wu, C. C., Ko, F. N., Kuo, S. C., Lee, F. Y., and Teng, C. M. (1995) *Br. J. Pharmacol. 116*, 1973−1978.
12. Wu, C. C., Ko, F. N., and Teng, C. M. (1997) *Biochem. Biophys. Res. Commun. 231*, 412−416.
13. Teng, C. M., Wu, C. C., Ko, F. N., Lee, F. Y., and Kuo, S. C. (1997) *Eur. J. Pharmacol. 320*, 161−166.
14. Friebe, A., Schultz, G., and Koesling, D. (1996) *EMBO J. 15*, 6863−6868.
15. Stone, J. R., and Marletta, M. A. (1998) *Chem. Biol. 5*, 255−261.
16. Friebe, A., and Koesling, D. (1998) *Mol. Pharmacol. 53*, 123−127.
17. Sharma, V. S., Magde, D., Kharitonov, V. G., and Koesling, D. (1999) *Biochem. Biophys. Res. Commun. 254*, 188−191.
18. Kuo, S.-C., Lee, F. Y., and Teng, C.-M. (1996) Yung Shin Pharm. Ind. Co., Ltd., United States Patent 5 574 168.
19. Brandish, P. E., Buechler, W., and Marletta, M. A. (1998) *Biochemistry 37*, 16898−16907.
20. Stone, J. R., and Marletta, M. A. (1994) *Biochemistry 33*, 5636−5640.
21. Callahan, P. M., and Babcock, G. T. (1981) *Biochemistry 20*, 952−958.
22. Choi, S., Lee, J. J., Wei, Y. H., and Spiro, T. G. (1983) *J. Am. Chem. Soc. 105*, 3692−3707.
23. Spiro, T. G., and Li, X.-Y. (1988) in *Biological Applications of Raman Spectroscopy* (Spiro, T. G., Ed.) pp 1−37, John Wiley & Sons, New York.
24. Tomita, T., Ogura, T., Tsuyama, S., Imai, Y., and Kitagawa, T. (1997) *Biochemistry 36*, 10155−10160.
25. Deinum, G., Stone, J. R., Babcock, G. T., and Marletta, M. A. (1996) *Biochemistry 35*, 1540−1547.
26. Fan, B., Gupta, G., Danziger, R. S., Friedman, J. M., and Rousseau, D. L. (1998) *Biochemistry 37*, 1178−1184.
27. Yu, A. E., Hu, S. Z., Spiro, T. G., and Burstyn, J. N. (1994) *J. Am. Chem. Soc. 116*, 4117−4118.
28. Schelvis, J. P., Zhao, Y., Marletta, M. A., and Babcock, G. T. (1998) *Biochemistry 37*, 16289−16297.
29. Gerzer, R., Böhme, E., Hofmann, F., and Schultz, G. (1981) *FEBS Lett. 132*, 71−74.
30. Stone, J. R., Sands, R. H., Dunham, W. R., and Marletta, M. A. (1995) *Biochem. Biophys. Res. Commun. 207*, 572−577.
31. Humbert, P., Niroomand, F., Fischer, G., Mayer, B., Koesling, D., Hinsch, K. D., Gausepohl, H., Frank, R., Schultz, G., and Böhme, E. (1990) *Eur. J. Biochem. 190*, 273−278.
32. Tian, W. D., Sage, J. T., and Champion, P. M. (1993) *J. Mol. Biol. 233*, 155−166.
33. Morikis, D., Champion, P. M., Springer, B. A., and Sligar, S. G. (1989) *Biochemistry 28*, 4791−4800.
34. Kim, S. Y., Deinum, G., Gardner, M. T., Marletta, M. A., and Babcock, G. T. (1996) *J. Am. Chem. Soc. 118*, 8769−8770.

35. Kushkuley, B., and Stavrov, S. S. (1996) *Biophys. J. 70*, 1214−1229.
36. Schelvis, J. P. M., Kim, S., Zhao, Y., Marletta, M. A., and Babcock, G. T. (1999) *J. Am. Chem. Soc. 121*, 7397−7400.
37. Li, X. Y., and Spiro, T. G. (1988) *J. Am. Chem. Soc. 110*, 6024−6033.
38. Lin, S. H., Yu, N. T., Tame, J., Shih, D., Renaud, J. P., Pagnier, J., and Nagai, K. (1990) *Biochemistry 29*, 5562−5566.
39. Kerr, E. A., Mackin, H. C., and Yu, N. T. (1983) *Biochemistry 22*, 4373−4379.
40. Yu, N.-T., and Kerr, E. A. (1988) in *Resonance Raman spectra of heme and metalloproteins* (Spiro, T. G., Ed.) pp 39−95, Wiley, New York.
41. Ray, G. B., Li, X. Y., Ibers, J. A., Sessler, J. L., and Spiro, T. G. (1994) *J. Am. Chem. Soc. 116*, 162−176.
42. Fan, B., Wang, J., Stuehr, D. J., and Rousseau, D. L. (1997) *Biochemistry 36*, 12660−12665.
43. Wang, J., Stuehr, D. J., and Rousseau, D. L. (1997) *Biochemistry 36*, 4595−4606.

BI992332Q